Supporting Information for

Three-Dimensional Electrode Characteristics and Size / Shape Flexibility for Coaxial-Fibers Bundled Batteries

Yoshinari Makimura, Chikaaki Okuda, Toshihisa Munekata, Azusa Tsukigase, Hideaki Oka, Tooru Saeki, Ryohei Morimoto, Megumi Sasaki, Hiroyuki Nakano, Yuichi Ito, Mamoru Mizutani, Tsuyoshi Sasaki

Toyota Central R&D Labs., Inc., Nagakute, Aichi 480-1192, Japan.

Corresponding Author

Email: ymakimura@mosk.tytlabs.co.jp.

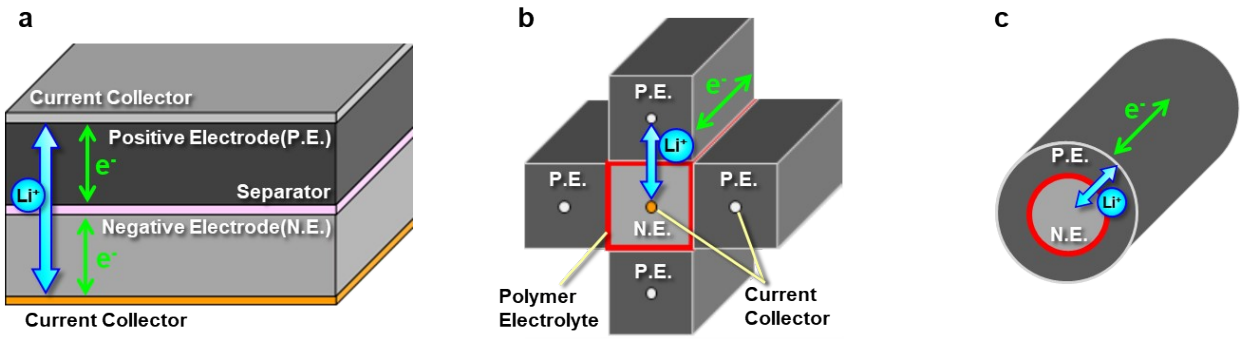

Figure S1. Schematic illustrations of achieving high electrode-area with high energy density by innovating the electrode geometry: (a) conventional sandwich-type internal structure in which positive and negative electrode sheets are stacked alternately with the separator; (b) cross-sectional image of a grid pattern of the positive and negative electrode rods arranged alternately; and (c) single coaxial-fiber electrode.

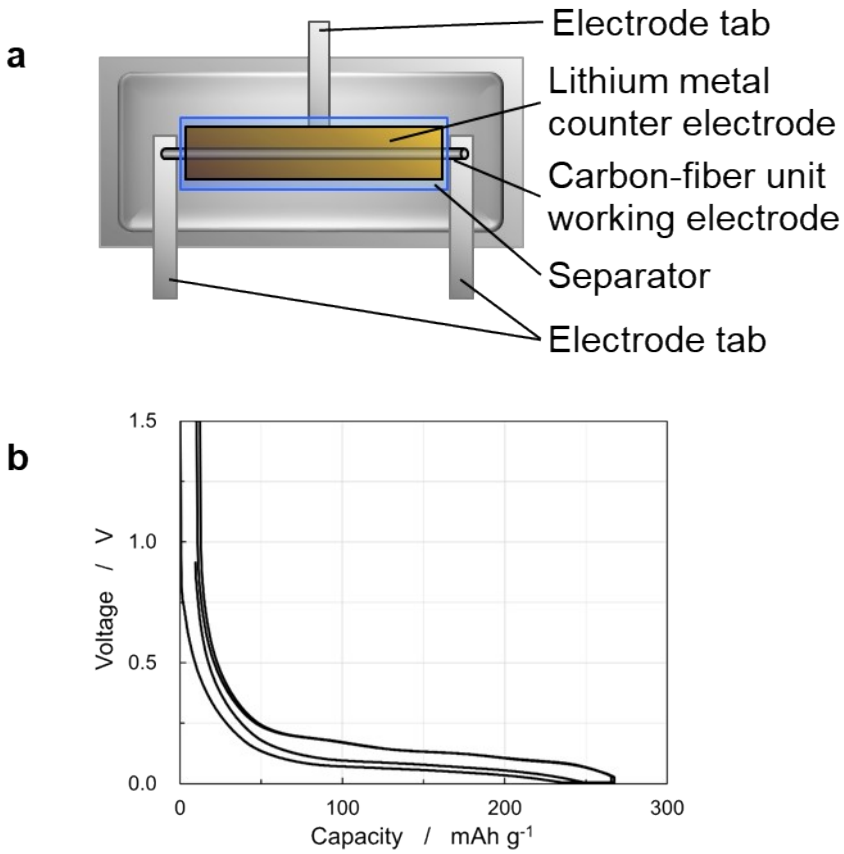

Figure S2. (a) Three-electrode pouch-cell with 130 mm long carbon-fiber unit sandwiched between 120 mm long lithium metal sheets from both sides via a polyethylene separator to examine electrochemical behavior and change in resistance at 1 kHz. (b) Voltage profiles of the pouch-cell's carbon-fiber unit.

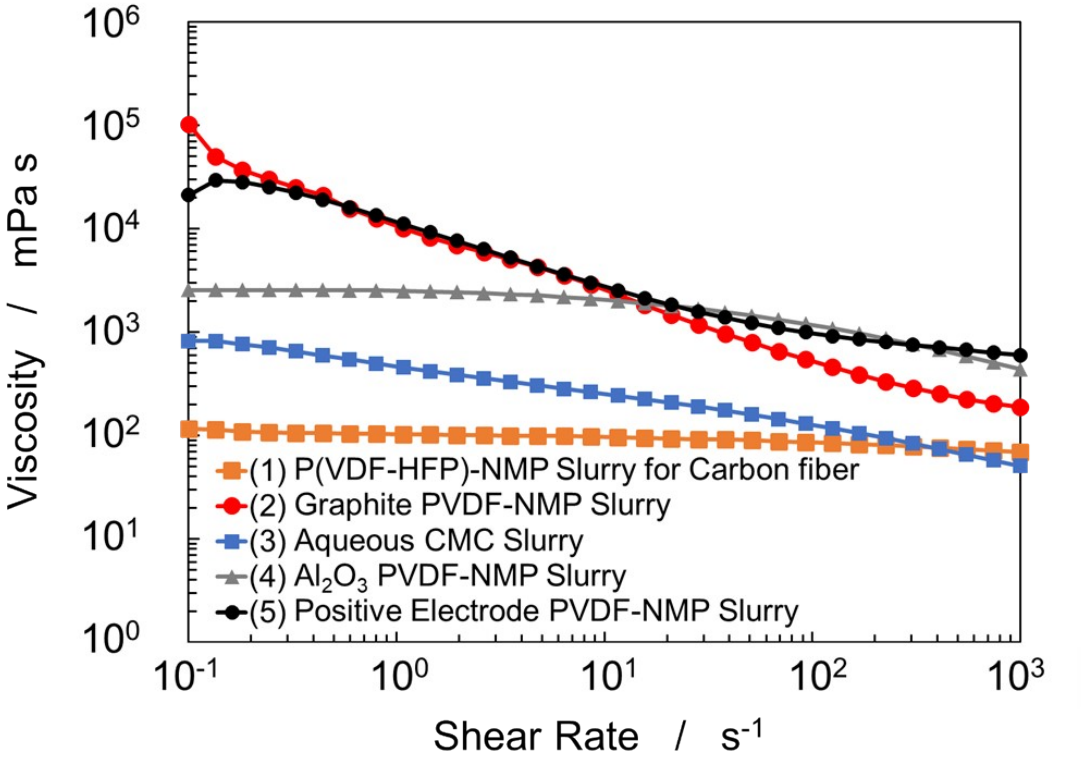

Figure S3. Viscosity for the slurries used for the electrodes or separator coating as a function of the shear rate to fabricate coaxial-fiber structure.

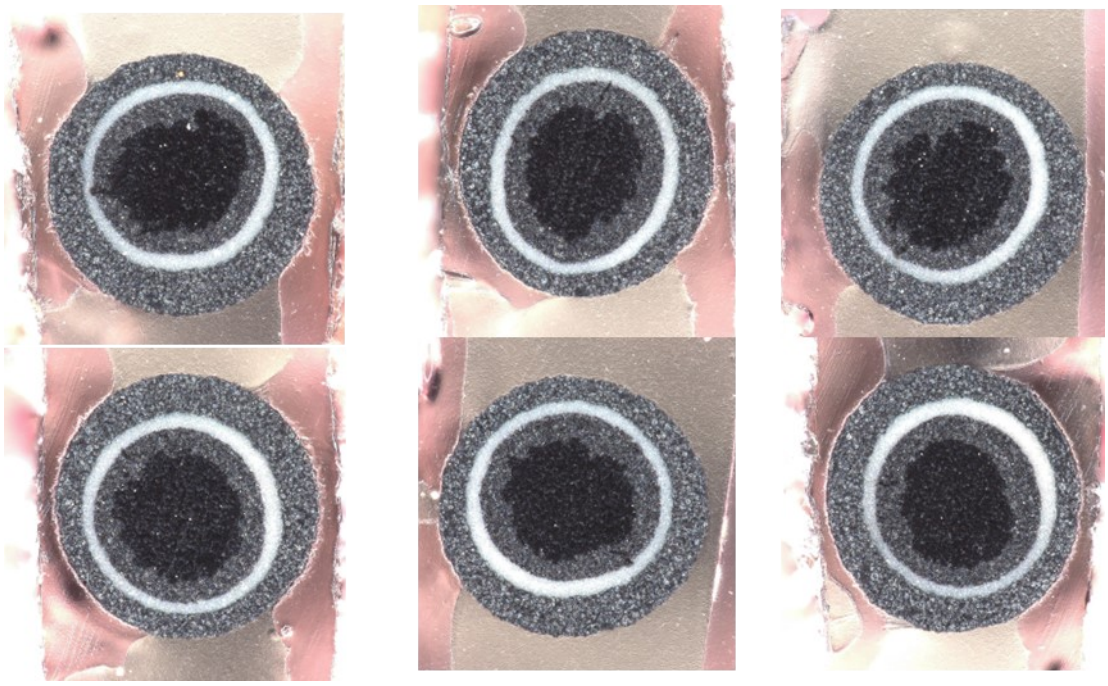

Figure S4. Cross-sectional images of a single coaxial-fiber electrode observed at several locations using an optical microscope.

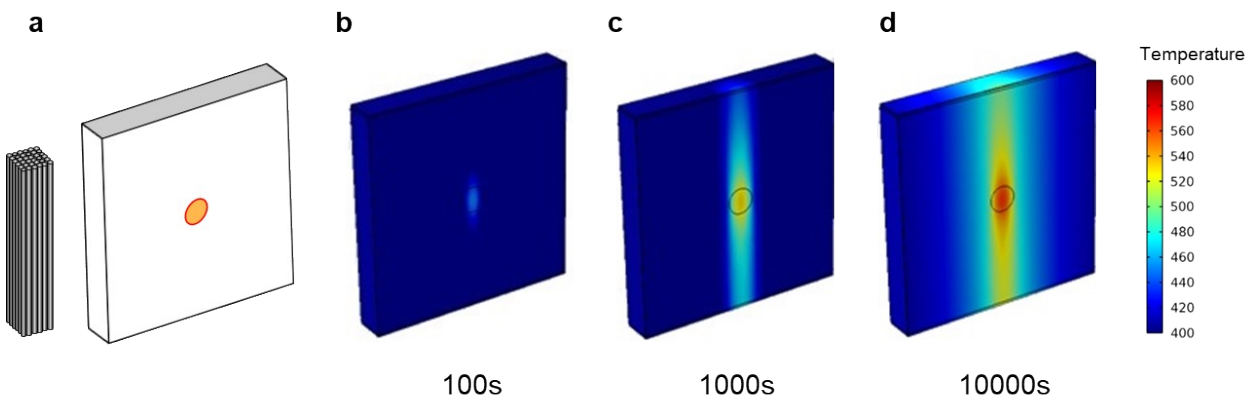

Figure S5. Battery model and simulated temperature distribution of the fiber-bundled structure

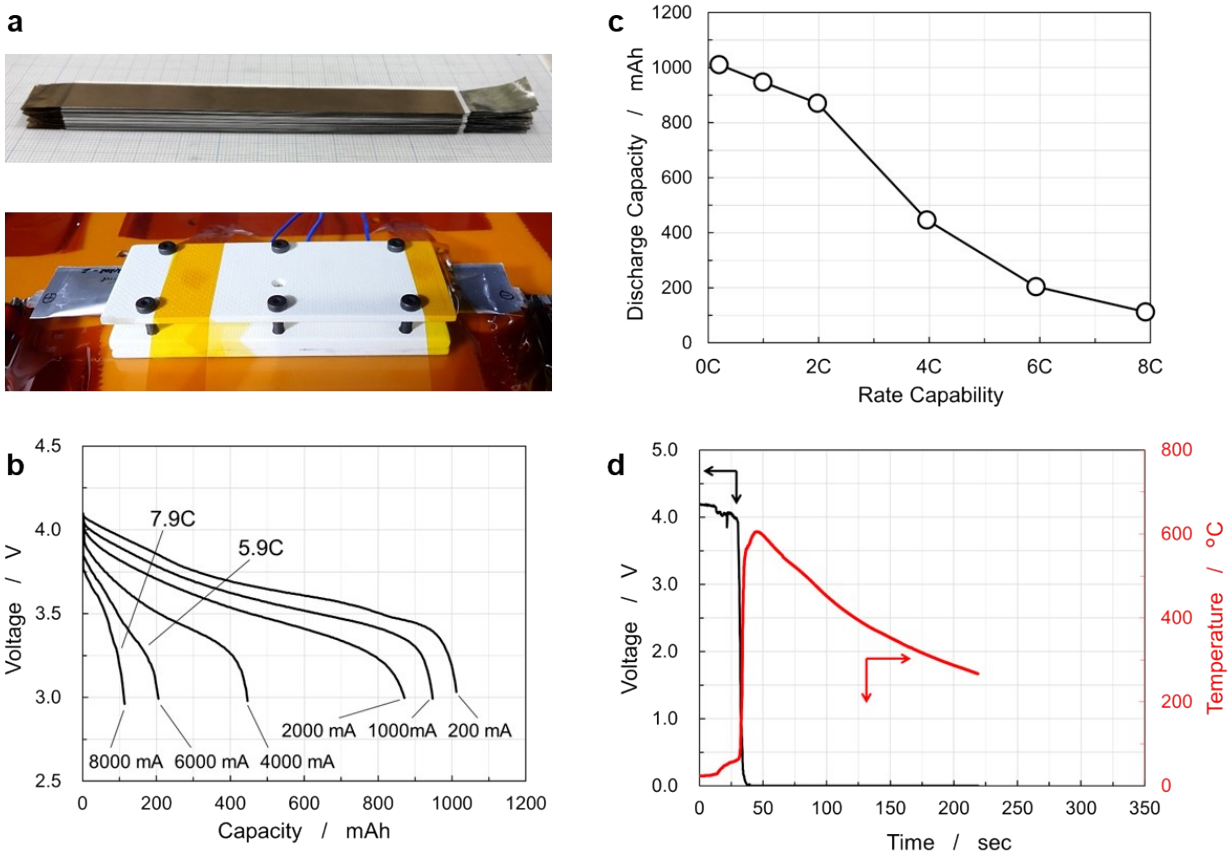

Figure S6. Sandwich-type multi-sheet battery: (a) photographs of the sandwich-type structure and the sealed battery; (b) discharge curves and (c) discharge capacity of the battery during a rate capability test; and (d) changes in voltage and temperature of the battery during the nail penetration test.

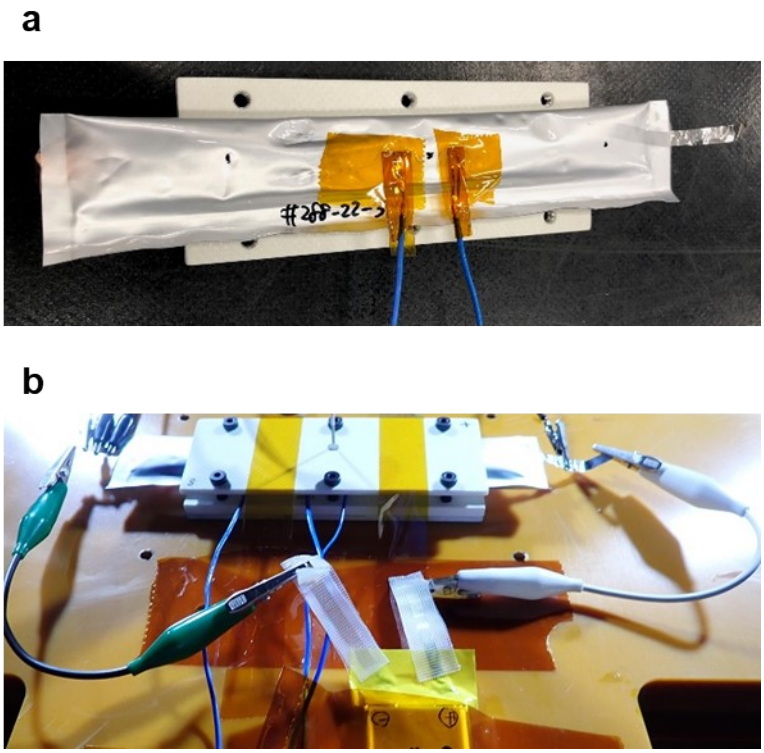

Figure S7. Photographs of the (a) CFBB consisting of 288 fiber electrodes and (b) experimental setup of the nail penetration test of the CFBB connected in parallel with 1100 mAh-class commercial lithium-ion battery.

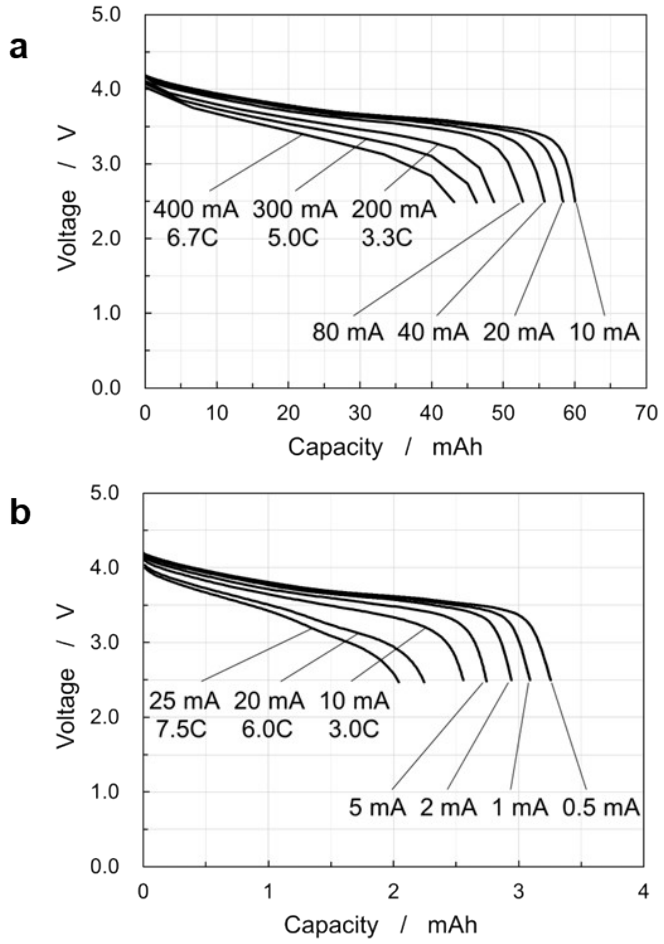

Figure S8. Discharge curves of 60 or 3.3 mAh-class CFBB during the rate capability test: (a) 60 mAh-class CFBB was charged at 10 mA to 4.2 V, held at the voltage for 2 h, and discharged at various currents from 10 to 400 mA at 20 ºC; (b) 3.3 mAh-class CFBB was charged at 1 mA to 4.2 V, held at the voltage for 2 h, and discharged at various currents from 0.5 to 25 mA at 20 ºC.

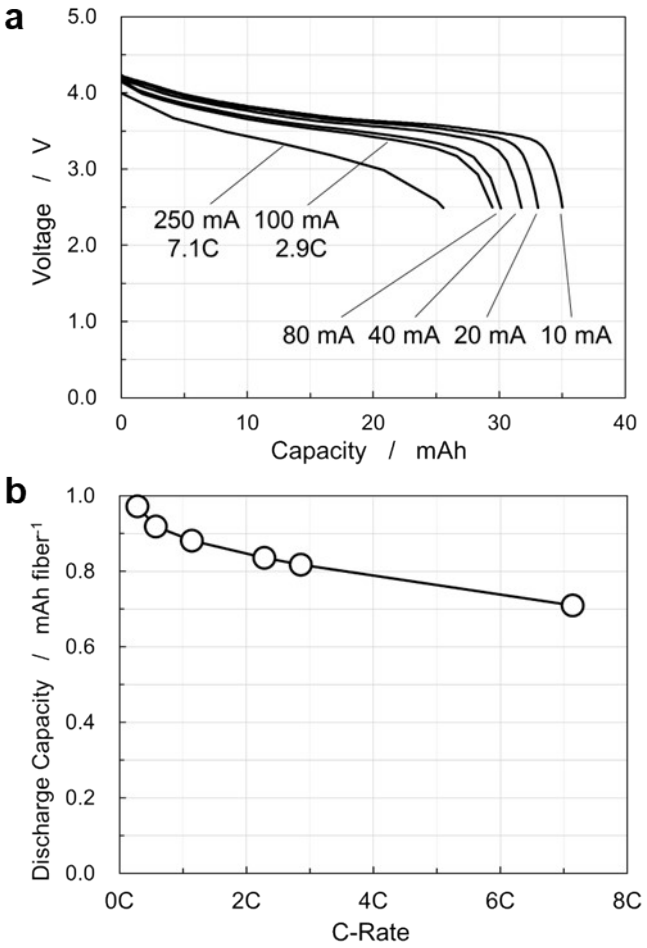

Figure S9. (a) Discharge curves of high energy-density CFBB consisting of 36 fiber electrodes during the rate-capability test. The cell was charged at 10 mA to 4.2 V, held at the voltage for 2 h, and discharged at various currents from 10 to 250 mA at 20 ºC. (b) Discharge capacities of the CFBB normalized by the values per a single coaxial-fiber electrode during the rate-capability test.

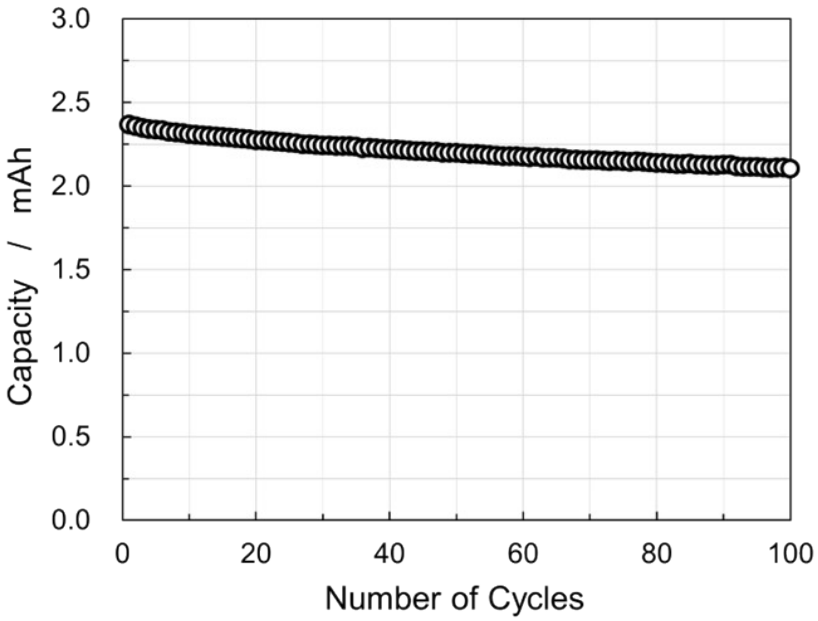

Figure S10. Capacity retention for the 3.3 mAh-class CFBB operated in a voltage window of 3.0–4.1 V at 0.7C-rate at 20 °C.

Supplementary Video 1. Drone flight with four 225 mAh-class coaxial-fiber bundled batteries (CFBBs).

Table S1. Electrode and battery-design parameters to estimate energy-densities and electrode-areas.

	Single Coaxial-Fiber Structure	Conventional Sandwich-Type Structure
Positive Electrode	Active Material / Acetylene black / PVDF (88 / 6 / 6; wt%)	
Active Material	$LiNi_{1/3}Co_{1/3}Mn_{1/3}O_2$	
Electrode Density	2.8 g cm^{-3}	
Current Collector	Aluminum Sheet (7μm x 0.5 x 0.25)	Aluminum Sheet (15 μm)
Discharge Capacity	150 mAh g^{-1}	
Operating Voltage	3.7 V vs. Li^+/Li	
Negative Electrode	Carbon Fiber	Graphite / Binder (98 / 2; wt%)
Active Material	Carbon Fiber	Graphite
Electrode Density	1.86 g cm^{-3}	1.6 g cm^{-3}
Current Collector	None	Copper Sheet (10 μm)
Thickness	20 – 500 μm (radius)	20 – 500 μm (thickness)
Discharge Capacity	330 mAh g^{-1}	
Operating Voltage	0.1 V vs. Li^+/Li	
Separator	Al_2O_3 / PVDF (90 / 10; wt%)	Polyethylene
Thickness	15 μm	15 μm
Electrolyte	1M $LiPF_6$ dissolved in EC / DMC / EMC (3 / 4 / 3 by volume) solution	
Capacity-Ratio of Negative to Positive Electrode	1.1	

Table S2. Sizes with standard deviation σ of each component in a single coaxial-fiber electrode.

Size (μm)	No. 1	No. 2	No. 3	No. 4	No. 5	No. 6	Average
Diameter of negative electrode	222.5	227.2	224.1	228.6	230.8	222.2	225.9
Standard deviation σ	19.9	15.7	23.0	24.9	24.0	36.8	
Thickness of separator	16.6	16.6	17.2	17.1	17.1	17.9	17.1
Standard deviation σ	2.9	2.1	3.2	3.4	3.3	4.9	
Thickness of positive electrode	49.6	44.2	46.9	44.6	44.0	44.0	45.6
Standard deviation σ	10.0	7.4	9.7	9.3	7.5	7.2	

Table S3. Size, weight, and energy density of the CFBBs. The weight of electrolyte in the CFBBs was calculated from the volume of voids within the CFBBs and the specific gravity of the electrolyte.

Number of fiber electrodes in CFBBs	Size of electrodes			Weight (g)	Discharge capacity (mAh)		Energy Density	
	Height (mm)	Width (mm)	Length (mm)		Battery	A single fiber electrode	Volumetric (Wh L^{-1})	Gravimetric (Wh kg^{-1})
4	0.326	0.938	98	0.078	3.3	0.830	410	158
18	0.349	4.139	98	0.349	14.0	0.856	403	163
72	1.280	4.523	98	1.398	60.1	0.834	392	159
288	4.903	4.474	98	5.447	222.1	0.771	382	151
36	0.583	4.597	98	0.673	35.0	0.973	493	192

Table S4. Energy densities and high-rate capabilities for commercial lithium-ion batteries.

Ref.	Model No.	Cell format	Capacity	Energy density		Maximum current	
				Volumetric	Gravimetric	Charging	Discharging
–	LP603449	Pouch	1100 mAh	414 Wh L^{-1}	185 Wh kg^{-1}	1.1 A (1C-rate)	2.2 A (2C-rate)
48	INR18650-MJ1	18650	3500 mAh	736 Wh L^{-1}	260 Wh kg^{-1}	3.4 A (1C-rate)	10 A (3C-rate)
						Capacity retention on 4C-rate charge at 25ºC	
49	INR18650-35E	18650	3367 mAh	715 Wh L^{-1}	251 Wh kg^{-1}	29%	
49	NCR18650GA	18650	3277 mAh	720 Wh L^{-1}	261 Wh kg^{-1}	25%	
49	INR21700-50E	21700	4921 mAh	722 Wh L^{-1}	259 Wh kg^{-1}	21%	
49	INR21700M50T	21700	4743 mAh	709 Wh L^{-1}	255 Wh kg^{-1}	22%	

Table S5. Estimated Joule heat and temperature rise of carbon fibers during high-rate discharge.

Number of fiber electrodes	Carbon fibers in CFBBs		Rate capability test				Joule heat (J)	Temp. rise (ºC)**
	Total Weight (mg)	Resistance (Ω)*	C-Rate	Current (mA)	Discharge Capacity (mAh)	Discharge time (sec)		
4	11.37	8.662	7.5C	25	2.04	294	1.59	197
18	51.16	1.925	6.6C	99	10.3	375	7.07	195
72	204.62	0.481	6.7C	400	43.1	388	29.88	206
288	818.50	0.120	7.6C	1700	180.4	382	132.85	229
36	102.31	0.962	7.1C	250	25.6	369	22.14	305

* The volume resistivity of the carbon fiber in the charged state of SOC50% was assumed to be 5.44 x 10^{-4} Ω cm since the volume resistivity of the carbon fiber was 3.4 x 10^{-3} Ω cm, and the 1 kHz resistance of the carbon fiber shown in Fig. 1(e) at SOC50% decreased to 16% of the initial value.

** The temperature rise of the carbon fiber in CFBBs was estimated by assuming the specific heat capacity of 0.71 J $g^{-1}K^{-1}$ equivalent to that of graphite.

Table S6. Charge and discharge currents of the rate-capability tests of coaxial-fiber bundled batteries (CFBBs) and their C-rates based on the discharge capacity at low-rate.

Number of fiber electrodes in CFBBs	Capacity mAh	Low-rate charge-discharge		Rate capability test	
		Charge mA (C-rate)	Discharge mA (C-rate)	Charge mA (C-rate)	Discharge mA (C-rate)
4	3.3	1 (0.3C)	0.5 (0.15C)	1 (0.3C)	0.5 (0.15C), 1 (0.3C), 2 (0.6C), 5 (1.5C), 10 (3.0C), 20 (6.0C), 25 (7.5C)
18	15	0.5 (0.03C)	0.5 (0.03C)	2 (0.13C)	1 (0.07C), 5 (0.3C), 10 (0.7C), 20 (1.3C), 40(2.7C), 60 (4.0C), 99 (6.6C)
				1 (0.07C), 5 (0.3C), 10 (0.7C), 20 (1.3C), 40 (2.7C), 60 (4.0C), 80 (5.3C), 99 (6.6C)	0.5 (0.03C)
72	60	10 (0.17C)	10 (0.17C)	10 (0.17C)	10 (0.17C), 20 (0.3C), 40 (0.7C), 80 (1.3C), 200 (3.3C), 300 (5.0C), 400 (6.7C)
288	225	20 (0.09C)	20 (0.09C)	20 (0.09C)	20 (0.09C), 50 (0.2C), 100 (0.4C), 400 (1.8C), 800 (3.6C), 1200 (5.4C), 1700 (7.6C)
36	35	10 (0.29C)	10 (0.29C)	10 (0.29C)	10 (0.29C), 20 (0.6C), 40 (1.1C), 80 (2.3C), 100 (2.9C), 250 (7.1C)